Alginate/Protamine/Silica Hybrid Capsules with Ultrathin Membranes for Laccase Immobilization

Ji-Yun Wang, Hai-Rong Yu, Rui Xie, Xiao-Jie Ju, Ya-Lan Yu, and Liang-Yin Chu
School of Chemical Engineering, Sichuan University, Chengdu, Sichuan 610065, P.R. China

Zhibing Zhang
School of Chemical Engineering, University of Birmingham, Edgbaston, Birmingham B15 2TT, U.K.

DOI 10.1002/aic.13834
Published online May 31, 2012 in Wiley Online Library (wileyonlinelibrary.com).

A novel type of core–shell capsules with ultrathin alginate/protamine/silica (APSi) hybrid membranes are successfully fabricated through a coextrusion minifluidic approach and a biosilicification method for immobilization of laccase. The ultrathin membranes were beneficial to the mass transfer across the capsule membranes, and the silica layer on the outer surface was efficient to inhibit the swelling of the capsule membranes. The immobilizing yield was considered to be 100% because all the enzyme molecules were encapsulated inside the capsules through the proposed method, and the laccase activity immobilized in APSi capsules was 61.8 mmol·g^{-1}·min^{-1}. The thermal, pH and storage stabilities of the immobilized laccase in APSi capsules were determined in comparison with free laccase. The stability of encapsulated laccase was significantly improved, which was as high as 67% after 20 days. The residual relative activity of encapsulated laccase remained 45% after 10 cycles. © 2012 American Institute of Chemical Engineers *AIChE J,* 59: 380–389, 2013
Keywords: enzyme immobilization, alginate/protamine/silica hybrid capsules, biomimetic capsules, silicification, laccase

Introduction

With the rapid development of biotechnology in recent years, enzyme technology including immobilization has been extensively applied in various fields, such as biocatalysis, biosensing, biopharmaceutics, and rapid disease diagnosis.[1–6] For *in vitro* applications of enzymes, their immobilization provides an effective approach to overcome some limitations of free enzymes.[7,8] For example, compared with free enzymes, immobilized enzymes are less sensitive to environmental stimuli, and can be removed from surrounding liquid and be recycled. Up to now, there have been mainly several types of enzyme immobilization methods, including physical adsorption, covalent bonding, crosslinking and embedding.[7–14] The embedding method immobilizes enzymes in hydrogels or encapsulates enzymes in semipermeable capsules,[10,14] which enable the bidirectional mass transfer across them, i.e., the inflow of reaction substrates and the outflow of products resulting from enzymatic reactions. In the case of embedding, enzyme properties could be improved by avoiding interaction with interfaces, or being influenced by the generation of a new environment, or by preventing enzyme subunit dissociation.[7,8]

To immobilize enzymes with the embedding method, the materials and structures of their carriers are very important to maintain their activity.[9,15] Nowadays, both natural polysaccharide polymers such as alginate, agar and chitosan and synthetic polymers such as polyacrylamide, poly(vinyl alcohol) and poly(lactic acid) have been used as the materials of carriers for immobilizing enzymes.[16–21] Because their networks are usually flexible, the polymeric carriers can easily swell due to the effect of inner osmotic pressure. As a result, some of the embedded enzymes can escape from the polymeric carriers when the swelling happens to the polymeric networks, and, thus, the enzyme immobilizing yield will be reduced to a certain extent. To prevent enzyme releasing from trapped enzyme preparations, some successful examples of immobilization of pre-immobilized or modified enzymes have been reported.[7] However, it is still desirable to search for new approaches which are effective to prevent untreated or unmodified enzymes escaping from their carriers. Therefore, under the precondition for the mass transfer of substrates and products, how to enhance the mechanical strength and inhibit the swelling of the carriers for enzyme immobilization is an important issue.

Inorganic materials, which are usually rigid, have been recently reported to form inorganic/organic hybrid carriers to reinforce the mechanical strength and inhibit the swelling behavior of the carriers for enzyme immobilization.[2,22–24] There have been mainly two methods to prepare inorganic–organic hybrid carriers for enzyme immobilization. One was a blending method, in which silica particles or precursors were blended with polymer solution, and then the polymeric components were crosslinked to form hybrid composites.[22,25,26] The other was a coating method, in which polymeric capsules were prepared first, then silica precursors

Additional Supporting Information can found in the online version of this article.

Current address of J.-Y. Wang: Chengdu Rongsheng Pharmaceuticals Co. Ltd., Chengdu, Sichuan 610041, P.R. China.
Correspondence concerning this article should be addressed to R. Xie at xierui@scu.edu.cn, and L.-Y. Chu at chuly@scu.edu.cn.

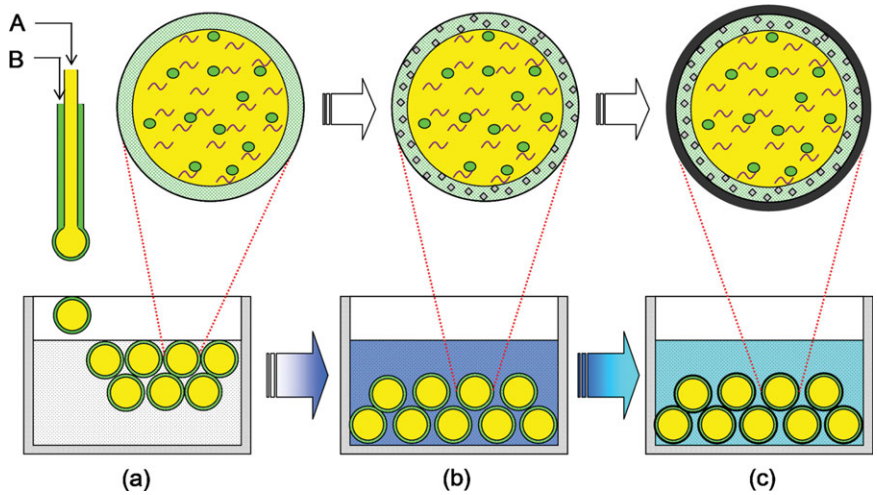

Figure 1. Schematic illustration of the process for fabricating the core–shell capsules with ultrathin alginate/protamine/silica (APSi) hybrid membranes through the coextrusion minifluidic approach and biosilicification method.

(a) Formation of Ca-alginate capsules with an ultrathin membrane in calcium nitrate solution by a co-extrusion minifluidic technique, (b) adsorption of protamine molecules onto the surfaces of Ca-alginate capsules in protamine solution, and (c) formation of a silica layer on the outer surface of capsules via silicification in sodium silicate solution. A: laccase solution with Na-carboxymethylcellulose (Na-CMC); B: Na-alginate solution. [Color figure can be viewed in the online issue, which is available at wileyonlinelibrary.com.]

were adsorbed onto the capsule surface, and finally a silica layer was synthesized on the outer surface to form hybrid capsule shells.[23,24,27] Recently, Zhang et al.[2,28] have proposed an attractive approach to prepare inorganic–organic hybrid capsule shells, in which they dripped calcium chloride ($CaCl_2$) droplets containing glucuronidase into a sodium alginate (Na-alginate) bath to form inner organic shells, then dipped the partially gelled capsules in a $CaCl_2$ bath to finish the gelation from the outside. After that, certain protamine molecules were absorbed onto the Ca-alginate shell, and then the protamine molecules inspired the silica formation on the outer surface of Ca-alginate capsules at 25°C and pH 7.0. Their results showed that the mechanical strength of the capsules was enhanced and the swelling was inhibited effectively by introducing the inorganic layer onto the outer surface of calcium alginate capsules.[2,28] However, the four-step process for preparing the hybrid capsules is still somewhat complex. Furthermore, the thickness of the hybrid capsule shell, which is one of the key factors determining the mass transfer of substrates and products across the capsule membrane, is still difficult to be controlled in the mentioned method. More recently, a simple coextrusion minifluidic approach to fabricate Ca-alginate capsules with aqueous core and an ultra-thin membrane[29,30] has been developed for decreasing the mass-transfer resistance across the capsule membrane, which may be extended to fabricate inorganic–organic hybrid capsules with ultrathin membranes for enzyme immobilization.

In this work, we prepared core–shell capsules with ultrathin alginate/protamine/silica (APSi) hybrid membranes through the coextrusion minifluidic approach and a biosilicification method for immobilization of a model enzyme laccase. The size and structure of the prepared capsules were characterized. Because laccase is able to oxidize both phenolic and nonphenolic lignin related compounds as well as highly recalcitrant environmental pollutants,[31] the immobilization of laccase was chosen in this study to investigate the carrier properties, aiming to realize a reusable application. The enzyme activity, and thermal, pH and storage stabilities of the immobilized laccase in APSi capsules were characterized, and compared with those of free laccase. Moreover, the residual relative activity of the encapsulated laccase in APSi capsules after being used for 10 cycles was determined.

Materials and Methods

Materials

Na-alginate was purchased from Tianjin Kemiou Chemical Reagent Development Center, China. Protamine sulfate salt from salmon (P4380), laccase from trametes versicolor (53739, $>$ 20 units/mg) and the 2,2′-N-bis(3-ethyl benzothiazolinone-6-sulfonic acid) diamine salt (ABTS, A1888, purity $\geq$ 98% (TLC)) were purchased from Sigma-Aldrich Chemical Co. Na-carboxymethylcellulose (Na-CMC), calcium nitrate ($Ca(NO_3)_2$), sodium silicate ($Na_2SiO_3{\cdot}9H_2O$) used as a silica precursor, acetic acid (HAc) and sodium acetate (NaAc) were obtained from Chengdu Kelong Chemical Reagent Co., China. All other chemicals were of analytical grade.

Fabrication of APSi hybrid capsules with ultrathin membranes for laccase immobilization

The APSi hybrid capsules with ultrathin membranes were fabricated in a three-step process, as illustrated in Figure 1. First, Ca-alginate capsules with a controllable ultrathin membrane were prepared by a coextrusion minifluidic technique.[29,30] The water-in-water droplets with mixed solution of laccase (0.5 g/L) and Na-CMC (10 g/L) as the inner core, and Na-alginate solution (20 g/L) as the outer shell were prepared via the capillary coextrusion minifluidic apparatus. In the experiment, the volumetric flow rates of the core solution and shell solution were 10 mL/h and 2.5 mL/h, respectively. The droplets were dripped into the $Ca(NO_3)_2$ bath (10 wt %) one by one, and the alginate shells were gelated by Ca^{2+} immediately. The prepared capsules were then removed from the $Ca(NO_3)_2$ solution, rinsed with HAc-NaAc buffer (0.2 mol/L, pH 7.0) for three times. Because all

the laccase molecules were encapsulated inside the capsules through the aforementioned method, the immobilizing yield was considered to be 100%.

Then, alginate/protamine capsules with encapsulated laccase were prepared by adsorbing protamine molecules onto the surfaces of the Ca-alginate capsules once the alginate capsules were prepared. Protamine sulfate salt was dissolved in HAc-NaAc buffer (0.2 mol/L, pH 7.0), and the concentration of protamine sulfate salt was selected as 3.0 g/L. The Ca-alginate capsules were immerged in the protamine solution for 30 min under mild stirring (100 rpm) using an electric stirrer to permit the protamine molecules to gradually adsorb onto the Ca-alginate shell via electrostatic attraction. The prepared alginate/protamine capsules were washed with HAc-NaAc buffer (0.2 mol/L, pH 7.0).

Next, the alginate/protamine capsules were immediately transferred into sodium silicate solution (60 mmol/L), which had been prepared by dissolving sodium silicate in 0.2 mol/L HAc-NaAc buffer and the pH value was adjusted to 7.0, and the mild silicification was performed on the capsule surfaces to fabricate the APSi hybrid shells at room temperature. The silicification lasted for 2 h. Finally, the fabricated APSi hybrid capsules were washed with HAc-NaAc buffer (0.2 mol/L, pH 7.0) twice and stored at 4°C for further characterization.

In order to systematically investigate the effects of the carrier microstructures on the performance of the immobilized enzyme, Ca-alginate spheres were also prepared by replacing the core solution with Na-alginate solution containing both laccase and Na-CMC in the same capillary apparatus, and then APSi spheres were obtained from the Ca-alginate spheres by the same silicification method, as schematically illustrated in Figure S1 in the additional Supporting Information. Both Ca-alginate spheres and APSi spheres were used for the enzyme immobilization as references.

Characterization of APSi hybrid capsules

The morphology of Ca-alginate capsules and spheres, as well as APSi hybrid capsules and spheres was characterized from their optical pictures taken by a digital camera. The size distributions of the prepared spheres and capsules were evaluated by a coefficient of variation (CV), which is defined by Eq. 1

$$\mathrm{CV} = 100\% \times \left(\sum_{i=1}^{N} \frac{(D_i - \overline{D_n})^2}{N-1} \right)^{\frac{1}{2}} \Bigg/ \overline{D_n} \qquad (1)$$

where D_i is the diameter of the ith particle (sphere or capsule) (m), N is the total number of the particles counted (—), and $\overline{D_n}$ is the arithmetic average diameter (m) of the counted particles. More than 200 particles were counted to determine their mean size and distribution.

The surface and cross-sectional structures of the prepared spheres and capsules in dry state were characterized using scanning electron microscopy (SEM; JSM-5900LV, JEOL, Japan). The particle samples for SEM were first freeze-dried for 24 h, then frozen in liquid nitrogen for 10 min, fractured mechanically, and finally sputter-coated with gold for 40 s before the scanning. Energy dispersive X-ray spectroscopy (EDX) in conjunction with field emission scanning electron microscopy (FE—SEM, S-3400, Hitachi, Japan) was employed to confirm the coating of silica shell on the APSi hybrid capsules. The chemical composition of APSi hybrid capsule shells was also measured with a Fourier transform infrared spectrometer (FTIR, IR Prestige-21, Shimadzu, Japan). The FTIR specimen was prepared by a freeze-drying method and using KBr disc technique.

Enzymatic conversion reaction and productivity

The enzymatic conversion reaction of ABTS substrate was catalyzed by equal amount of free or immobilized laccase. First, 335 μg free laccase and 30 APSi hybrid capsules encapsulating the same amount of laccase were put into a conical flask each containing 50 mL HAc-NaAc buffer (0.2 mol/L, pH 3.0). The conical flasks were tightly sealed, heated to 37°C and equilibrated for 10 min. Subsequently, the enzymatic conversion reactions were performed by adding 300 μL ABTS solution (0.01 mol/L), respectively. At regular intervals, the absorbance of ABTS free radicals in the medium was analyzed by using an UV-spectrometer at a wavelength of 420 nm. The conversion productivities were calculated by comparing the amount of ABTS free radicals in the medium with time and the original amount of ABTS in the feed, as shown in Eq. 2

$$\text{Productivity} = \frac{P_t}{P_0} \times 100\% \qquad (2)$$

where P_t and P_0 are the amount of ABTS free radicals in the medium at time t, and the original amount of ABTS in the feed, respectively.

In order to compare the effects of carrier structures on the enzyme performances, the Michaelis constant (K_m), and the maximum reaction rate (V_{max}) of both free laccase and immobilized laccase in the aforementioned four carriers were measured according to a well-established method.[32] 335 μg encapsulated laccase were first put into 50 mL HAc-NaAc buffer (0.2 mol/L, pH 3.0), then heated to 37°C and equilibrated for 10 min. The conversion reactions were carried out by adding different amounts of ABTS substrate (2.5–15 $\times$ 10^{-7} mol), and after 10 min the concentration of ABTS free radicals were analyzed. The Michaelis constant (K_m), and the maximum reaction rate (V_{max}), were calculated by the Lineweaver-Burk equation

$$\frac{1}{v} = \frac{K_m}{V_{\max}} \left(\frac{1}{[S]} \right) + \frac{1}{V_{\max}} \qquad (3)$$

where v is the reaction rate of ABTS free-radical ($\mathrm{mol \cdot L^{-1} \cdot min^{-1}}$), and (S) is the substrate concentration ($\mathrm{mol \cdot L^{-1}}$).

Swelling characteristics of enzyme carriers

To study the swelling characteristics of enzyme carriers during the conversion reaction process, Ca-alginate spheres and capsules, as well as APSi spheres and capsules were individually introduced into 50 mL HAc-NaAc buffer (0.2 mol/L, pH 3.0) containing 3 $\times$ 10^{-6} mol ABTS at 37°C, and each conversion reaction was performed for 2 days. The number of carriers in each experiment was 30. The swelling degree was evaluated by comparing the carrier diameter before (D_b), and after the enzymatic conversion reaction (D_a)

$$\text{Swelling degree} = \frac{(D_a - D_b)}{D_b} \times 100\% \qquad (4)$$

Optimum temperature and pH for the catalytic reaction

To ascertain the optimum temperature for the catalytic reactions, 30 APSi hybrid capsules containing encapsulated

laccase and 30 μg of free laccase were respectively put into 50 mL of HAc-NaAc buffer (0.2 mol/L, pH 3.0), which was then equilibrated at designed temperatures ranging from 10 to 60°C for 10 min. Subsequently, the catalytic reactions were carried out by adding 3×10^{-6} mol ABTS substrate. After 10 min, the concentrations of ABTS free radicals were determined by using an UV-spectrometer at 420 nm. The relative activities of free laccase and encapsulated laccase were calculated by Eq. 5

$$\text{Relative activity} = \frac{A_{\text{exp}}}{A_{\text{max}}} \times 100\% \tag{5}$$

where A_{exp} is the amount of ABTS free radicals in the medium catalyzed at each temperature, and A_{max} is the maximum one among all the A_{exp} values.

The optimum pH value for the conversion reaction was investigated by adding the same amount of free and immobilized laccase into 50 mL of HAc-NaAc buffers at different pH (0.2 mol/L, pH ranging from 2.0 to 7.0), which was then equilibrated at 37°C for 10 min. The subsequent measurement and calculation of the relative activities were the same as those for determining the optimum temperature.

Thermal and pH stabilities of immobilized enzymes

Thermal stabilities of immobilized enzymes were investigated by adding 30 APSi hybrid capsules with encapsulated laccase and 30 μg free laccase into 50 mL HAc-NaAc buffer (0.2 mol/L, pH 3.0), which was incubated at different temperatures (from 10 to 60°C) for an hour. The conversion reactions were then performed by adding 3×10^{-6} mol ABTS substrate at the same optimum conditions (37°C, pH 3.0) determined from the aforementioned experiments, and the concentrations of ABTS free radicals were measured using an UV-spectrometer after 10 min. The relative stability of free laccase and encapsulated laccase were calculated by Eq. 6

$$\text{Relative stability} = \frac{B_{\text{exp}}}{B_{\text{max}}} \times 100\% \tag{6}$$

where B_{exp} is the amount of ABTS free radicals produced by the laccase being incubated at each temperature, and B_{max} is the maximum one among all the B_{exp} values.

pH stabilities of the enzyme were also investigated by putting 30 μg of free laccase and 30 immobilized laccase capsules into 2.0 mL HAc-NaAc buffers with different pH (0.2 mol/L, pH ranging from 2.0 to 7.0), which was equilibrated at 37°C for an hour. Then, 48 mL HAc-NaAc buffer (0.2 mol/L, pH 3.0) was added to each flask, the pH value was then adjusted to 3.0, and finally the conversion reactions were performed at the optimum conditions (37°C, pH 3.0). The relative stability of free laccase and encapsulated laccase in buffers at different pH values were also calculated by Eq. 6.

Storage and recycling stability of immobilized enzymes

Free laccase solution and APSi hybrid capsules containing encapsulated laccase were stored at 4°C and pH 7.0. At regular intervals, 30 μg free laccase and 30 APSi hybrid capsules were added into 50 mL HAc-NaAc buffer (0.2 mol/L, pH 3.0), which was equilibrated at 37°C for 10 min. The conversion reactions were then induced by adding 3×10^{-6} mol ABTS substrate. The residual relative activities of free and encapsulated laccase were measured by analyzing the ABTS free radicals after 10 min. The relative storage activities of free and encapsulated enzymes were calculated by Eq. 7

$$\text{Relative storage activity} = \frac{C_n}{C_0} \times 100\% \tag{7}$$

where C_{n} and C_0 are the amount of ABTS free radicals catalyzed by the enzyme after being stored for n days, and that by fresh enzyme without any storage $n = 0$, respectively.

In this study, the encapsulated laccases in APSi hybrid capsules were recycled to catalyze the conversion reaction of ABTS substrate. APSi hybrid capsules containing encapsulated laccase were added into 50 mL HAc-NaAc buffer (0.2 mol/L, pH 3.0), which was equilibrated at 37°C for 10 min. The catalytic reaction was then carried out by adding 3×10^{-6} mol ABTS substrate. After 10 min, the concentration of ABTS free radicals was determined by an UV-spectrometer at 420 nm. Subsequently, the APSi hybrid capsules were filtered and washed three times with HAc-NaAc buffer (0.2 mol/L, pH 7.0) for further usage. Then, the capsules containing encapsulated laccases were immediately used to catalyze the next cycle of reaction. The relative recycling efficiency of encapsulated laccase was calculated by Eq. 8

$$\text{Relative recycling efficiency} = \frac{E_n}{E_1} \times 100\% \tag{8}$$

where E_{n} and E_0 are the amount of ABTS free radicals in the nth cycle and that in the first cycle, respectively.

Results and Discussion

Morphological and compositional analyses

Figure 2 shows the optical images and size distributions of Ca-alginate spheres and capsules prepared by the coextrusion minifluidic approach. The prepared spheres and capsules looked spherical, and the average diameters were 2.68 and 3.75 mm, respectively. The difference in the size was due to the effect of osmotic pressure of the core solution. The CV values of Ca-alginate spheres and capsules calculated by Eq. 1 were 3.62% and 3.60%, respectively. The results indicate that both Ca-alginate spheres and capsules were highly monodisperse.

During the silicification process, the transparent Ca-alginate capsules became opaque once they contacted with protamine solution, and then became white when further immersed into Na_2SiO_3 solution. As shown in Figure 3, the APSi hybrid capsules were also spherical, and the average diameter (ca. 3.34 mm) was slightly smaller than that of Ca-alginate capsules. The sizes of Ca-alginate capsules increased gradually in the buffer, however, the silicification reactions were initiated once the Ca-alginate capsules were obtained, and the formed silica shell inhibited the swelling of Ca-alginate capsules. Therefore, the average size of APSi hybrid capsules was smaller than that of Ca-alginate capsules. Figure 3a and b show the optical image and size distribution of APSi hybrid spheres, respectively. Obviously, the APSi hybrid spheres were more transparent than Ca-alginate spheres. The difference in transparency might be induced by the structure variation. The average size of APSi hybrid spheres was 2.84 mm, which was slightly larger than that of Ca-alginate spheres because of the coating of a silica layer. The CV values of APSi hybrid spheres and capsules were 3.44% and 4.30%, respectively, which indicate that the APSi spheres and capsules were also monodisperse.

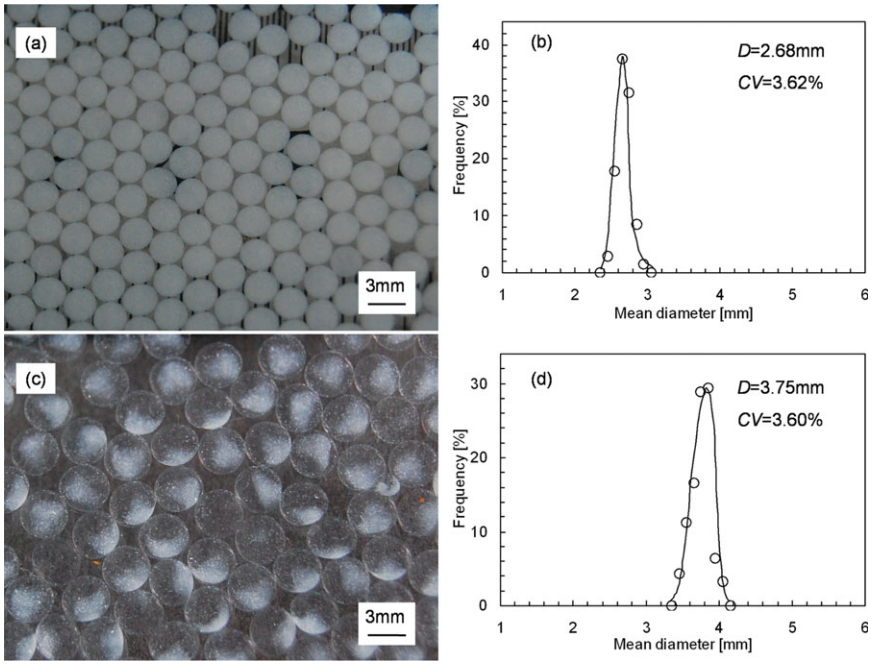

Figure 2. Optical images and size distributions of the prepared Ca-alginate spheres (a,b), and capsules (c,d).

[Color figure can be viewed in the online issue, which is available at wileyonlinelibrary.com.]

Figure 4 shows the SEM images of the cross-sectional views of Ca-alginate sphere, APSi hybrid sphere and capsule. In the sample preparation, the membrane of Ca-alginate capsules was too thin (fragile) to maintain intact structures after being freeze-dried so that no SEM images could be obtained for the cross-sectional views of Ca-alginate capsules. As shown in Figure 4c and e, both APSi hybrid sphere and capsule distinctly exhibit core–shell structures and a dense layer (coating) can be observed on the outer surface of the core. In comparison, the Ca-alginate sphere (Figure 4a and b) shows a three-dimensional (3-D) porous stromatolite structure from core to outer surface and no distinct dense shell. Such microstructure is beneficial to adsorb and immobilize a large amount of enzyme molecules due to its huge internal surface area. It is an interesting phenomenon that the APSi hybrid sphere exhibited a core–shell microstructure, which had continuous and uniform hybrid shell and no stromatolite structure like the Ca-alginate sphere. In the protamine solution, the Ca-alginate shell might adsorb protamine molecules on the surface. During the following silicification process, silica grew on the alginate/protamine shell and filled up the interstitial spaces among alginate and protamine molecules, resulting in

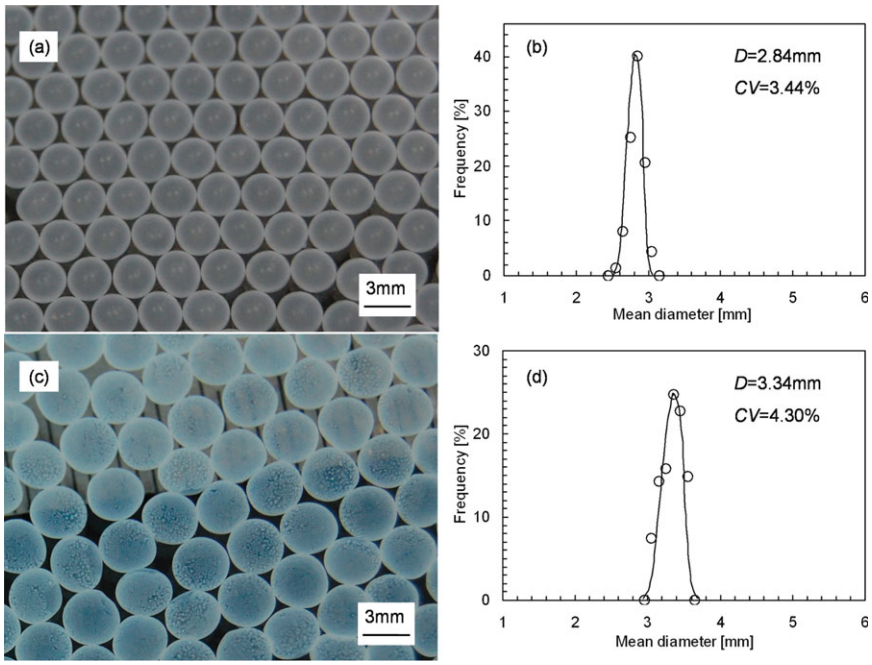

Figure 3. Optical images and size distributions of the prepared APSi hybrid spheres (a,b), and capsules (c,d).

[Color figure can be viewed in the online issue, which is available at wileyonlinelibrary.com.]

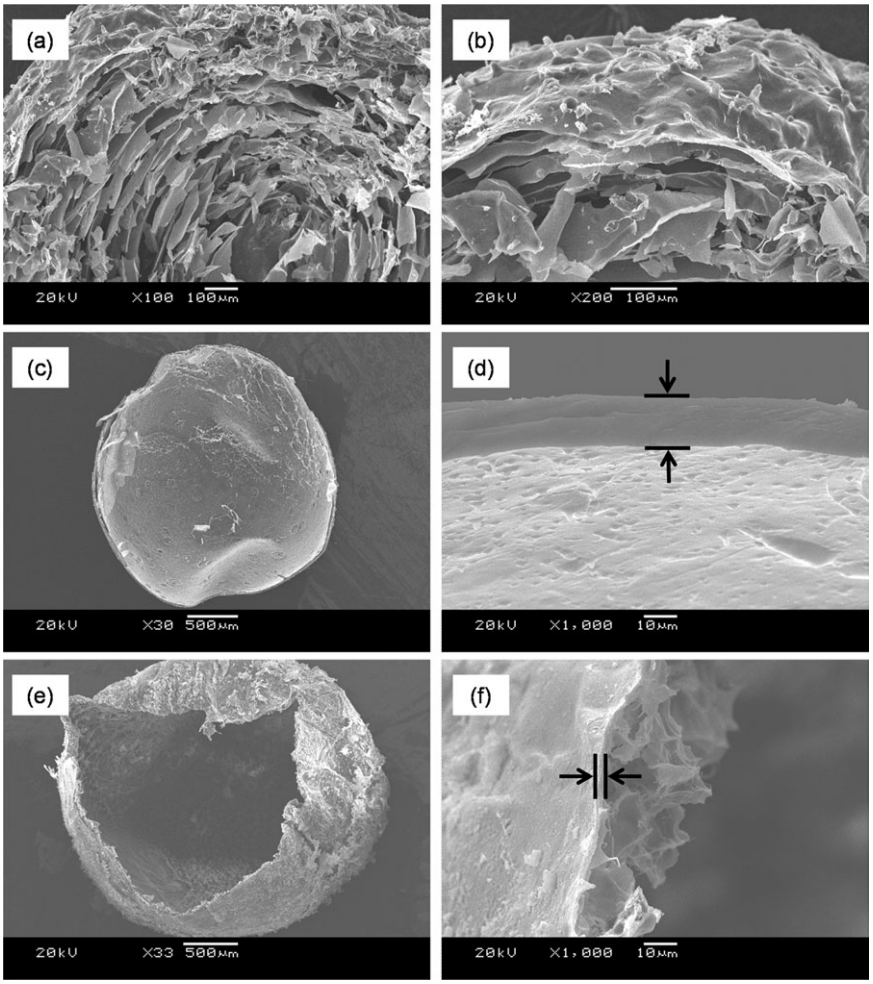

Figure 4. SEM images of the cross sections of Ca-alginate spheres (a,b), APSi hybrid spheres (c,d), and APSi hybrid capsules (e,f).

The thickness of the silica layer in (d), and (f) is marked by the arrows.

the continuous and uniform hybrid shell. At the same time, the Na^+ ions in the solution went into the shell, further loosened or even liquefied the Ca-alginate sphere by replacing the Ca^{2+} ions.[22,33] The shell thickness of the APSi hybrid sphere was about 15 μm. The average thickness of dense shell of the APSi hybrid capsule reduced significantly and was as thin as about 2.2 μm, which is more desirable for the mass transfer of substrates and products. Interestingly, there was a loose layer under the dense shell of the APSi hybrid capsule. The porous layer might be composed of alginate and protamine molecules, and the reason may be that the Ca-alginate capsule adsorbed less protamine molecules on the surface because of the lack of negatively charged groups than the Ca-alginate sphere did.

To further confirm the element composition of the APSi hybrid shells, EDX line scan analysis was employed. Figure

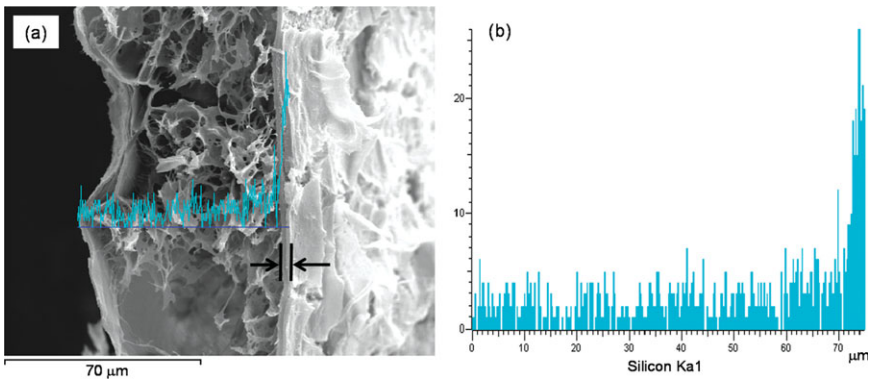

Figure 5. FE—SEM image (a), and EDX scan (b) of the cross section of an APSi hybrid capsule membrane.

The local line scan curve (light blue) presents the transmembrane distribution of Si element. [Color figure can be viewed in the online issue, which is available at wileyonlinelibrary.com.]

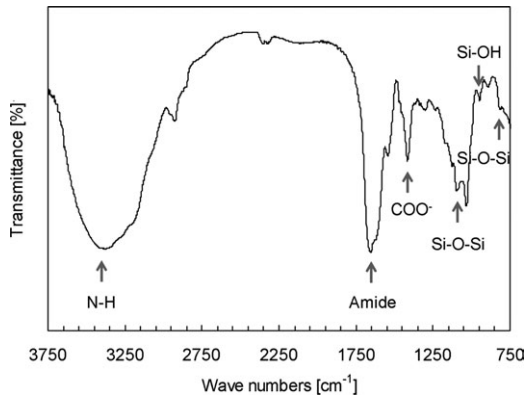

Figure 6. FTIR spectrum of the APSi hybrid capsule membranes.

5 exhibits the FE—SEM micrograph and EDX line scan result of the cross section of the APSi hybrid shell. The Si element (light blue) distributes throughout the cross section of the APSi hybrid shell, however, the concentration of Si element on the outer surface is remarkably higher than that on the loose layer. The results reveal that a silica shell was successfully synthesized on the surface of Ca-alginate capsule by the silicification process.

Figure 6 shows the FTIR spectrum of the APSi hybrid capsule shell. It not only shows the typical peaks of silica (Si—O—Si and Si—OH), but also peaks of protamine (N—H and amide) and alginate (COO—), indicating that the protamine was successfully introduced into the hybrid shell and the APSi hybrid shell was fabricated as desired.

Enzymatic conversion reaction and productivity

Figure 7 shows the productivity of ABTS free radicals with reaction time, converted by equal amount of free laccase and encapsulated laccase in the aforementioned four carriers. Obviously, the free laccase has the highest relative activity. The equilibrium productivity catalyzed by free laccase reached 90% after 3 min, while that in Ca-alginate capsules was 90% after 15 min. Furthermore, the productivity catalyzed by laccase immobilized in APSi capsules reached 87% after 30 min, which is lower than that in Ca-alginate capsules. To further illustrate the differences, the enzyme activities of free and encapsulated laccase were calculated and are listed in Table S1 in the Supplementary Information. The expressed laccase activities immobilized in Ca-alginate and APSi capsules are 129.9 and 61.8 $mmol \cdot g^{-1} \cdot min^{-1}$, respectively. Compared with that of free laccase, the relative activities in Ca-alginate and APSi capsules are 29.3% and 13.9%, which are considered to be acceptable for enzyme immobilization. The main reason for the decrease in the expressed enzyme activity in carriers is that the laccase is separated and parted with substrates after immobilization, and thus a longer time is needed for transbarrier permeation of substrates and products to achieve the catalytic reaction. For Ca-alginate and APSi capsules, the shell reduces the mass transfer rate of substrates and products; therefore, the expressed activity is reduced to some extent. Meanwhile, the productivity catalyzed by laccase in Ca-alginate spheres and APSi hybrid spheres reaches 25% after 30 min and 5% after 30 min, respectively. The Ca-alginate spheres are 3-D hydrogel networks and the silica shell of APSi spheres is as thick as about 15 μm so that the mass transfer rate is affected significantly; therefore, the catalytic reaction is significantly restrained. That is, although the expressed laccase activity immobilized in the APSi capsules is not so high, it is much greater than the expressed laccase activity immobilized in the APSi spheres, which clearly meets the objective of this work.

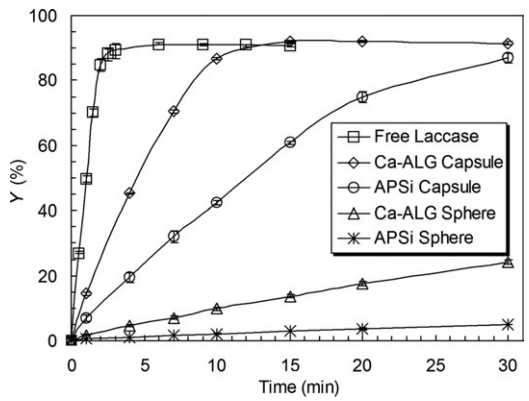

Figure 7. Effect of the carrier structure on the productivity of ABTS free radicals with reaction time.

Table 1. Kinetic Parameters for Free and Encapsulated Laccase

Laccase	K_m ($mmol \cdot L^{-1}$)	V_{max} ($mol \cdot L^{-1} \cdot min^{-1}$)
Free	0.1967	29.6077
Ca-alginate Capsules	0.2194	17.1274
APSi Capsules	0.2885	10.8732
Ca-alginate Spheres	0.3259	6.3715
APSi Spheres	0.5885	1.2145

The enzymatic conversion reaction of ABTS substance follows the Michaelis-Menten kinetics and the corresponding parameters, the Michaelis constant (K_m), and the maximum reaction rate (V_{max}), were calculated from Lineweaver-Burk plots (Eq. 3), and their values are listed in Table 1. The increase of K_m value after immobilization is mainly caused by the increased diffusion barrier as explained earlier, especially for the APSi spheres; as a result, the expressed activity is reduced to some extent. Due to the same reason, the maximum reaction rate (V_{max}) is also reduced after the immobilization. Because of the structural difference of carriers, the mass-transfer resistance for substrates and products across the carrier barrier is listed in order of magnitude from small to large as follows: Ca-alginate capsules $<$ APSi capsules $<$ Ca-alginate spheres $<$ APSi spheres; consequently, the V_{max} value of immobilized laccase in capsules is significantly higher than that in spheres.

Swelling characteristics

The swelling coefficient of polymeric particle is a characteristic parameter for evaluating its stability. The alginate carriers swelled significantly in solution, leading to the leakage of enzyme molecules. As shown in Figure 8, the swelling degree of Ca-alginate spheres is as high as 40%, and that of Ca-alginate capsules is approximately 20%. In this study, the silica shell was fabricated to inhibit the swelling behavior and prevent the loss of laccase. As expected, the swelling degrees of APSi hybrid spheres and APSi hybrid capsules were close to 0%, which indicates that there was no significant change in particle size during the enzymatic conversion reaction and the swelling behaviors have been completely inhibited after the coating of silica layer. Therefore, both APSi hybrid capsules and spheres significantly prevented the leakage of the enzyme. From the data of all of

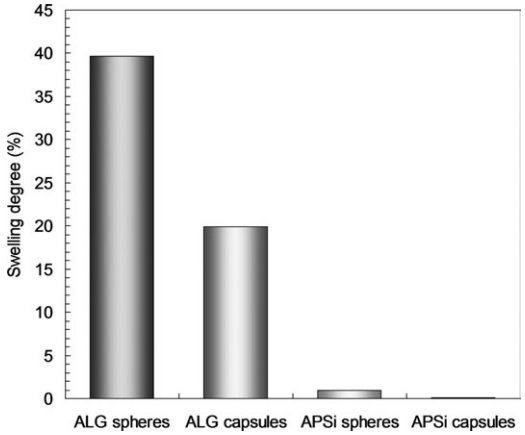

Figure 8. Swelling characteristics of different carriers for enzyme immobilization.

the enzymatic conversion productivity, Michaelis constant (K_m), the maximum reaction rate (V_{max}), and the swelling coefficient, the APSi hybrid capsules with ultrathin membranes were the best carriers for the laccase immobilization. Therefore, APSi hybrid capsules with ultrathin membranes were chosen for further investigations.

Optimum temperature and pH for enzymatic conversion

The relative catalytic activities of both free laccase and encapsulated laccase in APSi hybrid capsules with reaction temperature are shown in Figure 9a. The enzyme activity increases gradually with the surrounding temperature first, and as the temperature is higher than a certain value the activity decreases immediately due to the denaturing of the enzyme. As the temperature was above 60°C, most of the enzyme was denatured, resulting in a distinct decline of its catalytic efficiency. The optimum conversion temperature for free laccase is 37°C, while that for encapsulated laccase in APSi capsules is 40°C. Furthermore, the relative activity of the encapsulated laccase was almost always higher than that of free laccase for a given temperature. This might be attributed to the protection of the enzyme, provided by both the APSi hybrid shell and the liquid Na-CMC core solution.

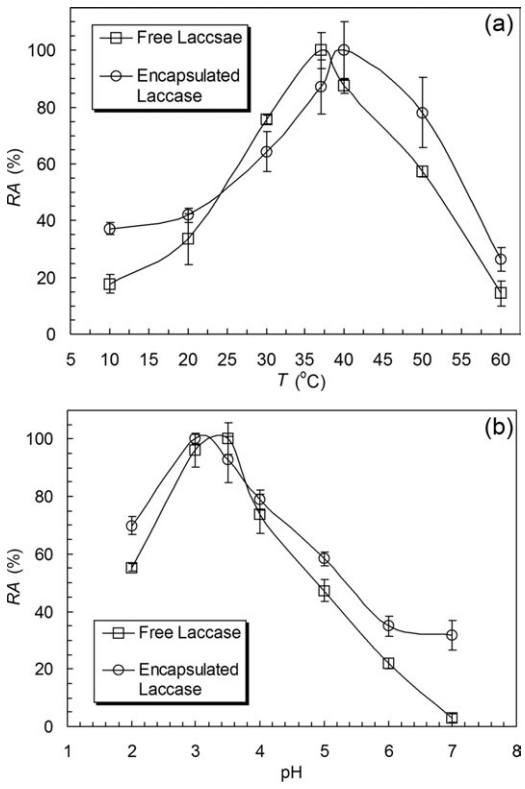

Figure 9. Effects of temperature (a), and pH (b) on the relative activities of free laccase and encapsulated laccase in APSi hybrid capsules.

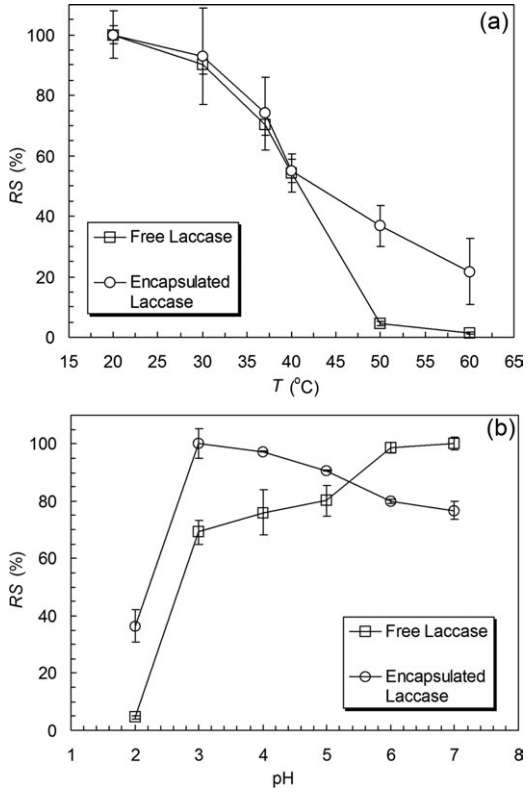

Figure 10. Thermal (a), and pH (b), stabilities of free laccase and encapsulated laccase in APSi hybrid capsules.

The relative activities of both free laccase and the encapsulated laccase in APSi capsules corresponding to different pH values are shown in Figure 9b. The highest activity of free laccase was obtained at pH 3.5, while that of encapsulated laccase in APSi capsules was obtained at pH 3.0. Compared with the free laccase, the encapsulated laccase in APSi capsules displayed a higher catalytic efficiency at pH varying from 2.0 to 7.0. This might be due to the protection of the enzyme by both APSi hybrid shell and the liquid Na-CMC core solution, which led to a less sensibility to ambient pH and a better catalytic activity. The results show that the encapsulated laccase in APSi capsules was more adaptable than free laccase, indicating that higher thermal and pH stabilities might be achieved by the encapsulation. To confirm this assumption, the thermal and pH stabilities of free and encapsulated laccase were also measured.

Thermal and pH stabilities of encapsulated laccase in APSi capsules

As shown in Figure 10, the encapsulated laccase in APSi capsules exhibits higher activity at temperatures of 20–60°C and pH 2.0–5.0 than the free laccase. With the increase of temperature or decrease of pH value, the relative activities

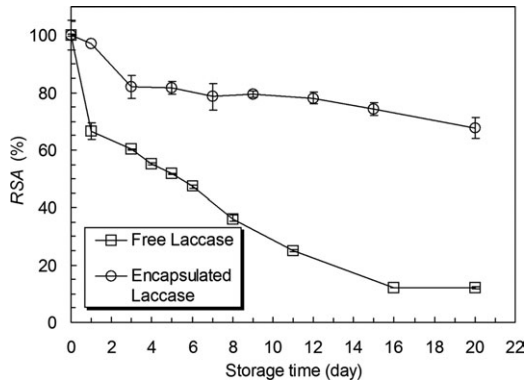

Figure 11. Storage stability of free laccase and encapsulated laccase in APSi hybrid capsules.

of both free and encapsulated laccase decrease gradually. However, for encapsulated laccase in APSi capsules, about 40% of enzyme activity remained after incubating at 50°C for 1 h, whereas only 5% of the free laccase activity remained after the same operation. Additionally, the encapsulated laccase displayed good pH stability at pH 3.0–7.0, but the relatively activity of free laccase was only about 65% at pH 3.0. This indicates that the thermal and pH stabilities of laccase have been improved significantly after being encapsulated in APSi capsules, due to the protection by APSi hybrid shells and Na-CMC core solution. The APSi hybrid shell inhibited the swelling to prevent loss of laccase from the liquid core. The electrostatic repulsive interaction between laccase and Na-CMC molecules and the suspending effect of Na-CMC molecules might also maintain effectively the conformation of laccase, and prevent it from disintegrating. It should be pointed that the optimum temperature of the encapsulated laccase in APSi capsules is 40°C (Figure 9), while the thermal stability at 40°C is lower than that at 37°C (Figure 10). Therefore, the operation temperature and pH of ABTS conversion reaction for encapsulated laccase in APSi capsules was selected as 37°C and 3.0, respectively in the subsequent experiments.

Storage and recycling stability of encapsulated laccase in APSi capsules

Both free and encapsulated laccase were stored at 4°C, and the data of the storage stabilities are shown in Figure 11. The relative catalytic activity of free laccase decreased rapidly to 66% after 1 day and went down continuously. 20 days later, only 12% of the enzyme activity remained. In contrast, the storage stability of the encapsulated laccase was significantly higher. The catalytic activity decreased by only 3% after 1 day storage. Although the activity also decreased with the increase of storage time, the remaining activity kept as high as 67% after 20 days. This may be considered to be due to protection by the liquid core solution and APSi hybrid shell. Both electrostatic repulsive interaction and suspending effect provided by Na-CMC molecules might effectively maintain the multilayer structures of laccase.

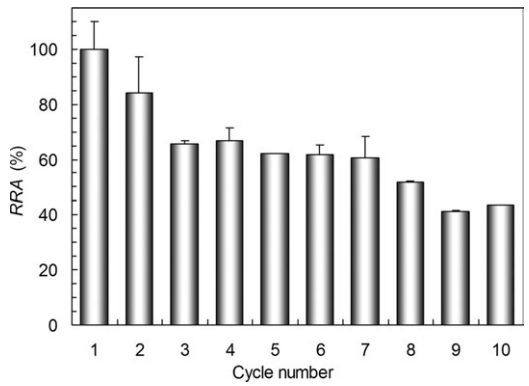

Figure 12. Recycling stability of encapsulated laccase in APSi hybrid capsules.

The recycling stability of the encapsulated laccase in APSi capsules is illustrated in Figure 12. Although the relative activity decreases remarkably in the first three cycles, it shows a good result in the following seven cycles, and about 45% of the enzyme activity remains in the 10th cycle. This may be because the electrostatic repulsion and suspending effect of the core solution prevented the laccase leaking. Additionally, the hybrid shell inhibited the swelling and improved the mechanical strength of APSi hybrid capsule during the recycle.

Conclusion

In this study, a novel type of core–shell APSi hybrid capsules with ultrathin membranes has been successfully developed for immobilization of laccase as a model enzyme. The prepared hybrid capsules were highly monodisperse, and the average diameter was about 3.34 mm. The APSi hybrid shells obviously inhibited the swelling of alginate carriers to prevent the laccase leaking. The optimum temperature and pH of the encapsulated laccase for ABTS substance were found to be 37°C and 3.0, respectively. Compared with free laccase, the immobilized laccase in APSi capsules had significantly higher thermal, pH and storage stabilities. The residual relative activity of the encapsulated laccase in APSi capsules still remained at 45% after 10 cycles. The preparation method of APSi hybrid capsules in this study may be extended as a general technique to yield a variety of promising products, such as microreactors, carriers for cell encapsulation and other enzymes.

Acknowledgments

This work was supported by the National Natural Science Foundation of China (20825622, 20906064, 21076127, 21136006), the National Basic Research Program of China (2009CB623407), the Program for Changjiang Scholars and Innovative Research Team in University (IRT1163), and the Foundation for the Author of National Excellent Doctoral Dissertation of P.R. China (201163). The authors gratefully thank Ms. Xin-Yuan Zhang in Analytical and Testing Center of Sichuan University for her help in the SEM imaging.

Literature Cited

1. Panke S, Wubbolts MG. Enzyme technology and bioprocess engineering. *Curr Opin Biotech*. 2002;13:111–116.
2. Zhang YF, Wu H, Li L, Li J, Jiang ZY, Jiang YJ, Chen Y. Enzymatic conversion of Baicalin into Baicalein by beta-glucuronidase encapsulated in biomimetic core-shell structured hybrid capsules. *J Molecul Catal B*. 2009;57:130–135.
3. Ivnitski D, Abdel-Hamid I, Atanasov P, Wilkins E. Biosensors for detection of pathogenic bacteria. *Biosens Bioelectron*. 1999;14:599–624.
4. Sun JJ, Zhu YH, Yang XL, Li CZ. Photoelectrochemical glucose biosensor incorporating CdS nanoparticles. *Particuology*. 2009;7:347–352.
5. Chan EC, Jiang F, Peshavariya HM, Dusting GJ. Regulation of cell proliferation by NADPH oxidase-mediated signaling: Potential roles in tissue repair, regenerative medicine and tissue engineering. *Pharmacol Therapeut*. 2009;122:97–108.

6. Natalio F, Link T, Muller WEG, Schroder HC, Cui FZ, Wang XH, Wiens M. Bioengineering of the silica-polymerizing enzyme silicatein-alpha for a targeted application to hydroxyapatite. *Acta Biomater*. 2010;6:3720–3728.
7. Rodrigues RC, Berenguer-Murcia A, Fernandez-Lafuente R. Coupling chemical modification and immobilization to improve the catalytic performance of enzymes. *Adv Synth Catal*. 2011;353:2216–2238.
8. Garcia-Galan C, Berenguer-Murcia A, Fernandez-Lafuente R, Rodrigues RC. Potential of different enzyme immobilization strategies to improve enzyme performance. *Adv Synth Catal*. 2011;353:2885–2904.
9. Mateo C, Palomo JM, Fernandez-Lorente G, Guisan JM, Fernandez-Lafuente R. Improvement of enzyme activity, stability and selectivity via immobilization techniques. *Enzyme Microb Tech*. 2007;40:1451–1463.
10. Sheldon RA. Enzyme immobilization: The quest for optimum performance. *Adv Synth Catal*. 2007;349:1289–1307.
11. Kurokawa Y. Entrap-immobilization of enzyme on composite gel fibre using a gel formation of cellulose acetate and metal (Ti, Zr) alkoxide. *Polym Gels Netw*. 1996;4:153–163.
12. Smith K, Silvernail NJ, Rodgers KR, Elgren TE, Castro M, Parker RM. Sol-gel encapsulated horseradish peroxidase: A catalytic material for peroxidation. *J Am Chem Soc*. 2002;124:4247–4252.
13. Subramanian A, Kennel SJ, Oden PI, Jacobson KB, Woodward J, Doktycz MJ. Comparison of techniques for enzyme immobilization on silicon supports. *Enzyme Microb Tech*. 1999;24:26–34.
14. Olea D, Viratelle O, Faure C. Polypyrrole-glucose oxidase biosensor - Effect of enzyme encapsulation in multilamellar vesicles on analytical properties. *Biosens Bioelectron*. 2008;23:788–794.
15. Cao LQ. Immobilised enzymes: science or art? *Curr Opin Chem Biol*. 2005;9:217–226.
16. Ichikawa S, Takano K, Kuroiwa T, Hiruta O, Sato S, Mukataka S. Immobilization and stabilization of chitosanase by multipoint attachment to agar gel support. *J Biosci Bioeng*. 2002;93:201–206.
17. Taqieddin E, Amiji M. Enzyme immobilization in novel alginate-chitosan core-shell microcapsules. *Biomaterials*. 2004;25:1937–1945.
18. Gonzalez-Saiz JM, Pizarro C. Polyacrylamide gels as support for enzyme immobilization by entrapment. Effect of polyelectrolyte carrier, pH and temperature on enzyme action and kinetics parameters. *Eur Polym J*. 2001;37:435–444.
19. Wang Y, Hsieh YL. Immobilization of lipase enzyme in polyvinyl alcohol (PVA) nanofibrous membranes. *J Membrane Sci*. 2008;309:73–81.
20. Wang X, Wenk E, Hu X, Castro GR, Meinel L, Wang X, Li C, Merkle H, Kaplan DL. Silk coatings on PLGA and alginate microspheres for protein delivery. *Biomaterials*. 2007;28:4161–4169.
21. Oddo L, Masci G, Di Meo C, Capitani D, Mannina L, Lamanna R, De Santis S, Alhaique F, Coviello T, Matricardi P. Novel thermosensitive calcium alginate microspheres: Physico-chemical characterization and delivery properties. *Acta Biomater*. 2010;6:3657–3664.
22. Coradin T, Nassif N, Livage J. Silica-alginate composites for microencapsulation. *Appl Microbiol Biot*. 2003;61:429–434.
23. Sakai S, Ono T, Ijima H, Kawakami K. Synthesis and transport characterization of alginate/aminopropylsilicate/alginate microcapsule: application to bioartificial pancreas. *Biomaterials*. 2001;22:2827–2834.
24. Kurayama F, Suzuki S, Oyamada T, Furusawa T, Sato M, Suzuki N. Facile method for preparing organic/inorganic hybrid capsules using amino-functional silane coupling agent in aqueous media. *J Colloid Interf Sci*. 2010;349:70–76.
25. Xu SW, Jiang ZY, Lu Y, Wu H, Yuan WK. Preparation and catalytic properties of novel alginate-silica-dehydrogenase hybrid biocomposite beads. *Ind Eng Chem Res*. 2006;45:511–517.
26. Coradin T, Livage J. Mesoporous alginate/silica biocomposites for enzyme immobilisation. *Comptes Rendus Chim*. 2003;6:147–152.
27. Sakai S, Ono T, Ijima H, Kawakami K. In vitro and in vivo evaluation of alginate/sol-gel synthesized aminopropyl-silicate/alginate membrane for bioartificial pancreas. *Biomaterials*. 2002;23:4177–4183.
28. Zhang YF, Wu H, Li J, Li L, Jiang YJ, Jiang Y, Jiang ZY. Protamine-templated biomimetic hybrid capsules: Efficient and stable carrier for enzyme encapsulation. *Chem Mater*. 2008;20:1041–1048.
29. Bremond N, Santanach-Carreras E, Chu LY, Bibette J. Formation of liquid-core capsules having a thin hydrogel membrane: liquid pearls. *Soft Matter*. 2010;6:2484–2488.
30. Wang JY, Jin Y, Xie R, Liu JY, Ju XJ, Meng T, Chu LY. Novel calcium-alginate capsules with aqueous core and thermo-responsive membrane. *J Colloid Interf Sci*. 2011;353:61–68.
31. Couto SR, Herrera JLT. Industrial and biotechnological applications of laccases: A review. *Biotechnol Adv*. 2006;24:500–513.
32. Robbins MH, Drago RS. Activation of hydrogen peroxide for oxidation by copper (II) complexes. *J Catal*. 1997;170:295–303.
33. Darrabie MD, Kendall WF, Opara EC. Characteristics of poly-L-ornithine-coated alginate microcapsules. *Biomaterials*. 2005;26:6846–6852.

Manuscript received Jan. 25, 2012, revision received Mar. 27, 2012, and final revision received May 2, 2012.